Radiological Evaluation of 510 Cases of Basilar Invagination with Evidence of Atlantoaxial Instability (Group A Basilar Invagination)

Atul Goel[1,2], *Sonal Jain*[1], *Abhidha Shah*[1]

■ OBJECTIVE: **To evaluate the musculoskeletal and soft tissue neural alterations in cases with group A basilar invagination.**

■ METHODS: **Between January 2007 and August 2016, 510 patients with group A basilar invagination were surgically treated. The radiologic images of these patients were reviewed retrospectively. The patients were divided into 4 groups: group A1, comprising 60 patients with syringomyelia; group A2, comprising 354 patients with "external syrinx," marked by excessive cerebrospinal fluid (CSF) in the extramedullary space; group A3, comprising 51 patients with both syringomyelia and external syrinx; and group A4, comprising 45 patients with no abnormality of CSF cavitation in the spinal canal.**

■ RESULTS: **A number of musculoskeletal and neural parameters, including the extent of basilar invagination, degree of angulation of the odontoid process, and facet malalignment, were evaluated in each of the 4 groups. The degree of basilar invagination was 6—27.4 mm (average, 15.85 mm) in group A1, 4.3—24.5 mm (average, 12.56 mm) in group A2, 5.6—17.6 mm (average 10.8 mm) in group A3, and 5.2—17.3 mm (average, 11.74 mm) in group A4. The angle of inclination of the odontoid process was 61.1—90.7 degrees (average, 71.4 degrees) in group A1, 30.5—79.8 degrees (average, 60.05 degrees) in group A2, 68.5—78.3 degrees (average, 73.4 degrees) in group A3, and 62.2—87.4 degrees (average, 71.2 degrees) in group A4.**

■ CONCLUSIONS: **The nature of bone malformations directly influences the presence or absence of external syrinx and syringomyelia.**

INTRODUCTION

The subject of basilar invagination has been evaluated for more than a century.[1-7] The continuous developments in the understanding of the subject and the hunt for optimum surgical treatment is one of the more fascinating success stories of modern medicine.[1] Biomechanical understanding, radiologic revolution, anatomic clarity, and clinical experience have combined to make this subject that was considered only a radiologic and clinical curiosity 50 years ago to one of the more rewarding surgical experiences today. Our personal understanding of the subject has evolved over the last 35 years of practice.[6-10]

A classification system introduced in 2004 divided cases with basilar invagination into 2 groups.[7] Group A basilar invagination is characterized by atlantoaxial instability, manifested by an abnormal increase in the atlantodental or clivodental interval, along with migration of the odontoid process into the foramen magnum according to the classical parameters described by Chamberlain and Wackenheim. In Group B basilar invagination cases, there was basilar invagination when assessed by parameter of Chamberlain but there was no evidence of atlantoaxial instability when assessed by the parameter of abnormal increase in atlantodental or clivodental interval and abnormal transgression of the Wackenheim's clival line by the odontoid tip.

In the present study, we evaluated the radiologic features of 510 patients with group A basilar invagination. We focused particularly

Key words
- Atlantoaxial dislocation
- Basilar invagination
- Chiari formation
- Syringomyelia

Abbreviations and Acronyms
CSF: Cerebrospinal fluid
CT: Computed tomography
MRI: Magnetic resonance imaging

From the [1]Department of Neurosurgery, King Edward Memorial Hospital and Seth G.S. Medical College, and [2]Department of Neurosurgery, Lilavati Hospital and Research Centre, Mumbai, India

To whom correspondence should be addressed: Atul Goel, M.Ch. [E-mail: atulgoel62@hotmail.com]

Citation: World Neurosurg. (2018) 110:533-543.
http://dx.doi.org/10.1016/j.wneu.2017.07.007

Journal homepage: www.WORLDNEUROSURGERY.org

Available online: www.sciencedirect.com

on the presence of syringomyelia and "external syrinx" and of syringobulbia and "external syringobulbia." The term "external syrinx" here refers to the presence of excessive cerebrospinal fluid (CSF) occupying the larger space in the widened subarachnoid spaces, and not to loculated tumor-like space-occupying collection as is seen in arachnoid cysts. Although other terms, including "external hydromyelia," "extramedullary hygroma," "spinal cord atrophy," "neural agenesis," and "external hydrocephalus or cyst," were considered to identify the presence of excessive CSF outside the spinal cord, external syringomyelia seems to best convey the intended meaning and was used in our earlier publications.[8,9] In parallel, the term "external syringobulbia" describes the presence of excessive CSF outside the confines of the brainstem and cerebellar convexity.

In the present study, we evaluated the relationship between musculoskeletal and soft tissue neural alterations, particularly as it relates to the development of CSF cavitations in the spinal canal and the brain.

METHODS AND RESULTS

During the period January 2007—August 2016, 620 patients with basilar invagination (groups A and B) were surgically treated in the Neurosurgery Departments of our institutions. Of these, 510 patients had group A basilar invagination and are the subject of the present radiologic evaluation. The remaining 110 patients had group B basilar invagination.[7] We investigated the radiologic features of group B patients in a previous study.[8] Magnetic resonance imaging (MRI) and computed tomography (CT) scans were available for review in all patients and were used to evaluate the radiographic parameters. Dynamic images with the head placed in flexion and extension positions of either plain radiograph, CT scan and/or MRI were available for review in 300 patients. Morphometric measurements of the dorsal spine were possible in 45 patients and of the lumbar spine in 11 patients. The preoperative radiologic images were evaluated retrospectively and were compared with a control cohort of 25 patients who were age- and sex-matched, had normal spinal architecture, had been investigated for unrelated causes, and had no craniovertebral or spinal abnormality or anomaly. A larger control cohort was not considered necessary, given that the normal values have been validated in previous studies.[6,8]

Depending on the type of CSF cavitation/loculation within or outside the spinal cord, the patients were divided into 4 subgroups (Table 1). Group A1 (60 cases) included the patients with syringomyelia (Figure 1). Group A2 (354 cases) included patients with external syrinx (Figures 2 and 3). Group A3 (51 cases) comprised patients with both syringomyelia and external syrinx (Figure 4). Group A4 (45 cases) included patients with no abnormality of CSF cavitation in the spinal canal (Figure 5). Syringobulbia was identified in 5 patients, and external syringobulbia was identified in 401 patients. All 5 patients with syringobulbia were in group A1. External syringobulbia was seen in 11 patients in group A1, 316 in group A2, 39 in group A3, and 35 in group A4. Chiari formation was seen in 126 patients, including 40 patients in group A1, 39 in group A2, 32 in group A3, and 12 in group A4.

Table 2 summarizes the epidemiologic data. Radiologic measurements were obtained in the 4 groups individually and compared with those of the normal cohort (Tables 3—5). The radiologic parameters were measured by 2 observers independently; there was no significant interobserver variation. Table 3 summarizes the bone and soft tissue anomalies, including Chiari formation, assimilation of the atlas, C2-3 fusion, bifid arches of the atlas, and subaxial bone fusions (Klippel—Feil abnormality). Cord girth measurements were used not to quantify the volume of the spinal cord, but rather to delineate the thickness of the column of the neural tissue in relation to the thickness of the column of CSF. Anteroposterior spinal canal and spinal cord girth measurements were made by sagittal MRI, with the mid-C6, mid-D4, and mid-L3 vertebral body levels as the index sites. In patients with syringomyelia, the neural girth was calculated as the sum of the measurements of neural tissues both anterior and posterior to the syrinx cavity. The spinal canal and neural girth measurements in the 4 groups are presented in Table 5.

Table 1. Classification of Group A Basilar Invagination

Classification	Number of Patients (%)
A1: internal syringomyelia	60 (12)
A2: external syringomyelia	354 (69)
A3: both internal and external syringomyelia	51 (10)
A4: no cord abnormality	45 (9)

With the patient in a neutral head position, a horizontal line (line A) is drawn connecting the tuberculum sellae to the inion. Line B is drawn parallel to line A and courses over the tip of the odontoid process. Line C is drawn parallel to line B and courses over the midpoint of the base of the C7 vertebra. The distance between lines A and B is considered the posterior cranial fossa height, and the distance between lines B and C is considered the neck height[11] (Figure 6). The anteroposterior dimension of the posterior cranial fossa is measured as the distance between the dorsum sellae and the internal occipital protuberance on the mid-sagittal cut of the CT scan. The length of the clivus is measured from the tip of the dorsum sellae to the lower edge of the clivus. A clivus <3.5 cm is considered short; 81 patients had a short clivus. The minimum craniocervical neural girth was measured at the level of tip of the odontoid process.

The Wackenheim clival line is drawn from the tip of the posterior clinoid process and extends along the posterior limit of the clivus.[12] Platybasia was assessed by measuring the basal angle, a line drawn from the nasion to the dorsum sellae and the Wackenheim clival line. The Chamberlain line is drawn from the posterior tip of the hard palate to the posterior rim of the foramen magnum.[13] Basilar invagination is considered severe when the tip of the odontoid process is >10 mm above the Chamberlain line. A total of 320 patients had severe basilar invagination.

The degree of neural compression was assessed by the tilt of the odontoid process toward the neural structures and measured using the modified omega angle.[6] A modified omega angle was measured with the patient's head in a neutral position (Figure 7). A line was drawn along the hard palate. Because C2-3 fusion was a frequent observation, line B was drawn

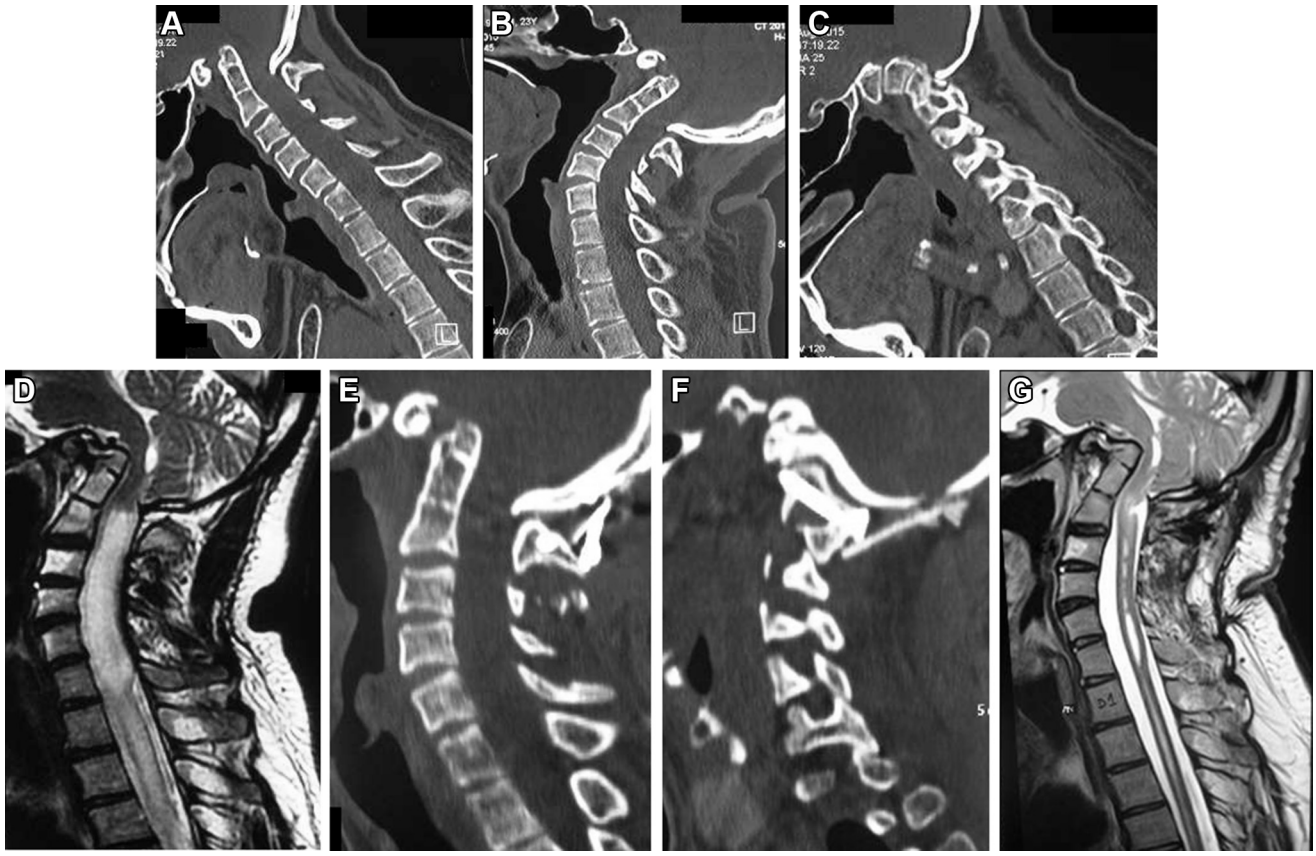

Figure 1. Group A1: Images of a 22-year-old male patient. (**A**) Computed tomography (CT) scan with the head in flexion showing basilar invagination. Assimilation of atlas and C2-3 fusion can be seen. (**B**) CT scan with the head in extension showing a mild reduction in basilar invagination. (**C**) CT scan, sagittal image, with the cut passing through the facets. Type A atlantoaxial facetal instability can be seen. (**D**) T2-weighted magnetic resonance imaging (MRI) showing syringomyelia and Chiari formation. Note the presence of external syringobulbia. (**E**) Postoperative CT scan showing reduction of atlantoaxial instability and fixation. (**F**) Postoperative CT scan cut though the facets showing the implant. (**G**) Delayed postoperative MRI (9 months after surgery) showing a reduction in the size of the syrinx.

parallel to line A and passed through the midpoint or center of the base of C3 (instead of the base of C2 as described earlier).[6] Line C was drawn from the midpoint of base of C3 body and extended superiorly along the tip of the odontoid process. The angle subtended between lines B and C was considered the inclination of the odontoid process in an anteroposterior perspective. The angle subtended between the Wackenheim clival line and a line drawn along the odontoid process (line C) was defined as craniovertebral angulation. Bimastoid or bidigastric lines were drawn on coronal images of either CT scans or MRI images. The angle subtended by the line drawn from the midpoint of the base of the C3 vertebra to the tip of the odontoid process on either of these lines was considered the inclination of the odontoid process in a transverse perspective. The C1 facetal angle was measured as the angle between a line drawn along the articular surface of the C1 facet and the horizontal in a neutral head position. The C2 facetal angle was measured as the angle between a line drawn along the articular surface of the C2 facet and the horizontal. The C1-2 coronal joint angulations were not evaluated, given that a significant number of patients had spondyloptosis of the atlantoaxial joint.

Mobile and partially reducible atlantoaxial dislocation (24 cases) was identified by alteration of atlantodental or clivodental (in cases with assimilation of atlas) interval on dynamic flexion-extension images. Mobile vertical atlantoaxial instability (47 cases) was diagnosed when the odontoid process moved relative to the anterior arch of the atlas (or the anterior rim of the foramen magnum in cases with assimilated atlas) on dynamic flexion-extension images. In accordance with a recently described classification of atlantoaxial instability based on facetal alignment in the neutral head position, basilar invagination was divided into 3 types: type A facetal instability (483 patients), with the facet of the atlas dislocated anterior to the facet of the axis; type B facetal instability (17 patients), with the facet of the atlas dislocated posterior to the facet of the axis; and type C facetal instability (10 patients), with the facets in alignment and the instability detected only on direct handling of bones during surgery.[14,15]

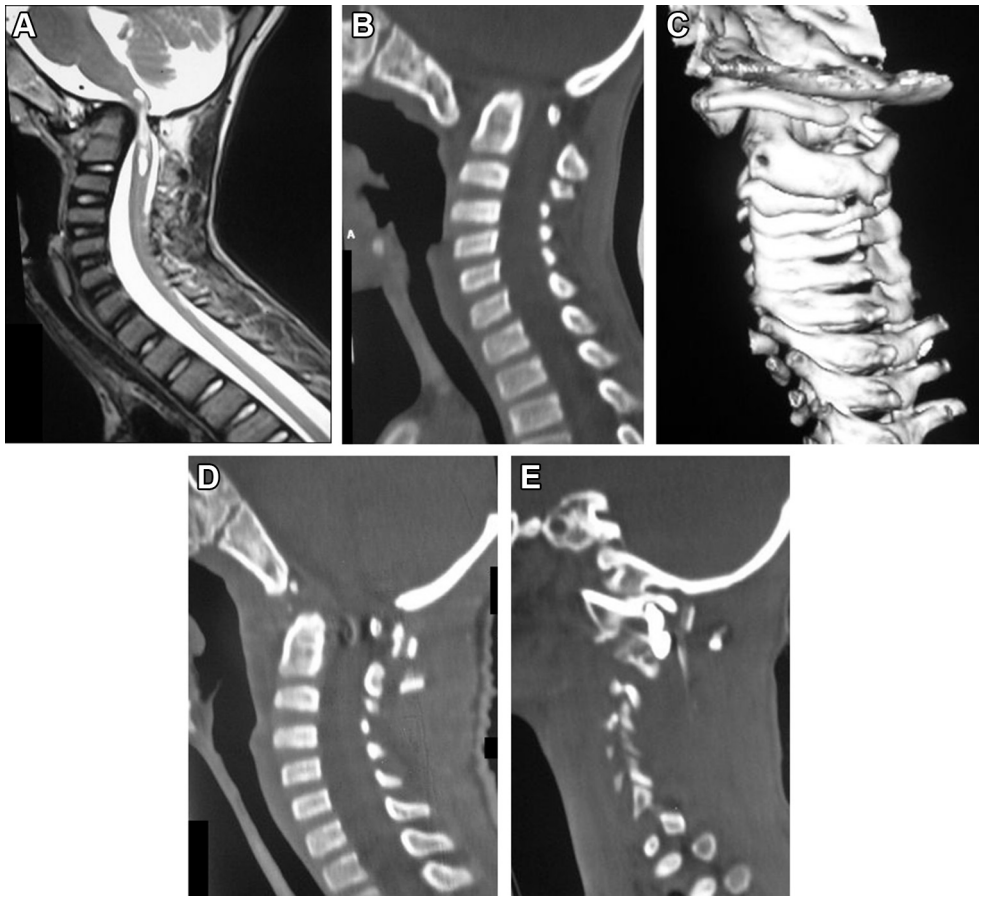

Figure 2. Group A2: images of a 7-year-old male. (**A**) T2-weighted magnetic resonance imaging showing basilar invagination and cord compression. External syringomyelia and external syringobulbia can be observed. (**B**) Computed tomography (CT) scan showing basilar invagination. (**C**) 3D CT scan showing type A atlantoaxial facetal instability. The bifid posterior arch of atlas can be observed. (**D**) Postoperative CT scan showing reduction of basilar invagination and fixation. (**E**) Postoperative CT scan with the cut passing through the facets showing the implant.

Statistical Analysis

Statistical analysis was performed using a 1-tailed *t* test. Significance was set at $P < 0.05$. The basal angle, craniovertebral angle, inclination of the odontoid (modified omega angle), posterior fossa height, and anteroposterior diameter of the posterior fossa of the 4 groups were compared with the control group, and the results were analyzed.

The basal angle was found to be more obtuse in all 4 groups of basilar invagination compared with the control group; the differences were statistically significant, at $P < 0.00001$ in group A1, $P < 0.0001$ in group A2, $P = 0.01793$ in group A3, and $P = 0.000554$ in group A4. The craniovertebral angle was more acute in all 4 groups compared with the control group. The mean angle in the control group was 143.4 degrees, compared with 104.6 degrees in group A1 ($P < 0.00001$), 106.9 degrees in group A2 ($P < 0.0001$), 104.7 degrees in group A3 ($P < 0.00021$), and 109.9 degrees in group A4 ($P < 0.00001$), a statistically significant difference for all 4 groups. There was no statistically significant difference in the posterior fossa height between any group and the control group. The mean posterior fossa height in the control group was 3.73 cm, compared with 3.17 cm in group A1 ($P = 0.069$), 3.74 cm in group A2 ($P = 0.20$), 3.77 cm in group A3 ($P = 0.29$), and 3.8 cm in group A4 ($P = 0.12$). The anteroposterior length of the posterior fossa was greater in all 4 groups compared with the control group. This greater length was statistically significant in groups A1, A2, and A4. The mean anteroposterior diameter in the control group was 8.3 cm, compared with 9.47 cm in group A1 ($P = 0.048$), 8.63 cm in group A2 ($P = 0.001$), 8.67 cm in group A3 ($P = 0.192$), and 8.81 cm in group A4 ($P = 0.00004$).

The modified omega angle was compared in the 4 groups and the control group. The difference in inclination of the odontoid process was statistically significant for groups A2, A3, and A4 ($P < 0.00001$, 0.0052, and 0.000164, respectively) but not for group A1 ($P = 0.053$). This finding suggests that the more acute inclination of the odontoid with the horizontal influences the development of

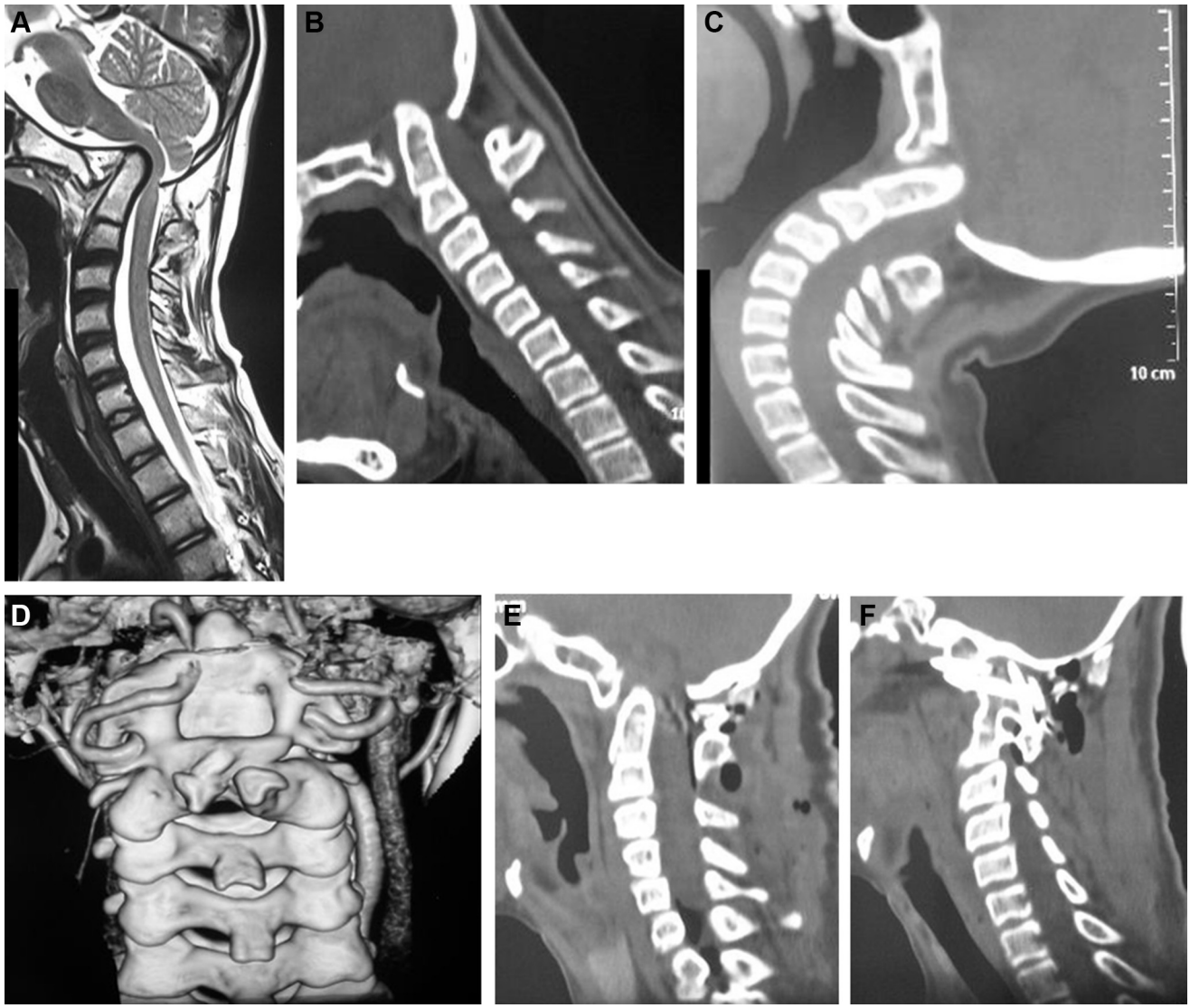

Figure 3. Group A2: Images of a 14-year-old male. (**A**) T2-weighted magnetic resonance imaging showing basilar invagination. Assimilation of the atlas and C2-3 fusion can be seen, along with external syrinx and external syringobulbia. (**B**) Computed tomography (CT) scan with the head in flexion showing basilar invagination. (**C**) CT scan with the head in extension showing a reduction in vertical atlantoaxial dislocation. (**D**) 3D CT scan showing the abnormal course of vertebral artery posterior to the facet of the atlas. (**E**) Postoperative CT scan showing a reduction of basilar invagination. (**F**) Postoperative CT scan showing the fixation construct.

external syringomyelia in patients with group A basilar invagination.

DISCUSSION

The classification of basilar invagination into 2 groups (A and B) identifies group A as a discrete clinical entity in which the atlantoaxial joint is unstable. In group A basilar invagination, the odontoid process seems to invaginate into foramen magnum or, as von Torklus noted in 1972, the spine migrates or herniates into the brain.[3] In group B, in contrast, the entire craniovertebral junctional zone is positioned rostrally. Essentially, for the first time in the literature we discussed the issue of instability at the atlantoaxial joint for the entity of basilar invagination that was considered to have a 'fixed' atlantoaxial joint. The study concluded that in patients with group A basilar invagination, the atlantoaxial joint is not only not fused or fixed, but also is excessively or abnormally mobile. More importantly, it was proposed that stabilization of the unstable joint and restoration of craniovertebral alignment can be the optimum surgical treatment in this subgroup of patients. From decompressive bone removal surgery by an anterior transoral route or by

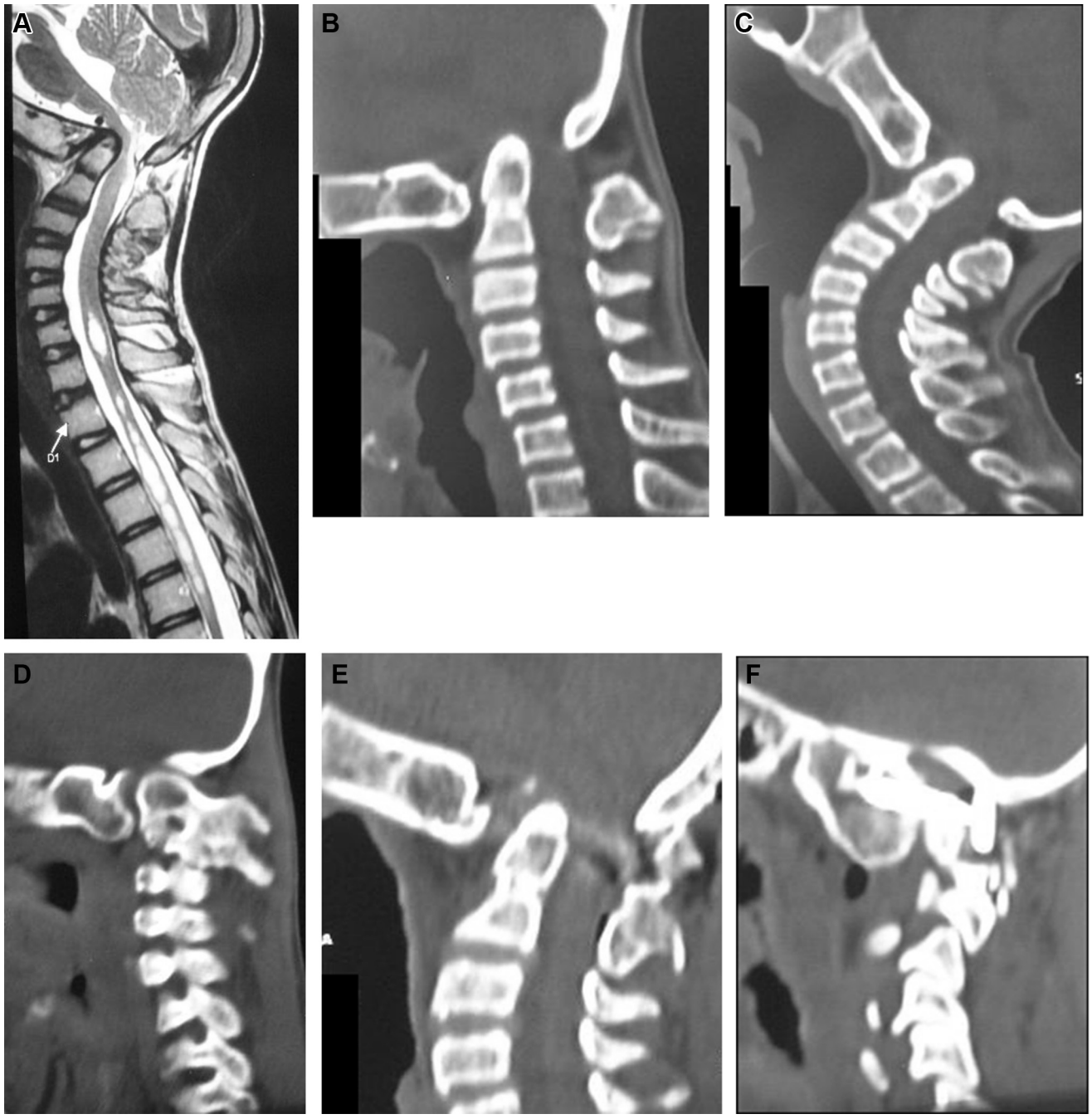

Figure 4. Group A3: Images of a 13-year-old male. (**A**) T2-weighted magnetic resonance imaging showing basilar invagination. Syringomyelia and external syringomyelia can be seen. (**B**) Computed tomography (CT) scan with head in flexion showing basilar invagination and assimilation of the atlas. (**C**) CT scan with the head in extension shows reduction in vertical atlantoaxial dislocation. (**D**) CT scan with the sagittal cut passing through the facets. The facet of atlas is dislocated anterior to the facet of the axis (spondyloptosis). (**E**) Postoperative CT scan showing reduction of dislocation and fixation. (**F**) Postoperative CT scan with cuts passing through facets showing the implant.

posterior foramen magnum decompression, the surgical treatment now involves facetal distraction and facetal fixation to provide craniovertebral realignment, and the procedure is aimed at arthrodesis of the atlantoaxial joint.[16,17] "Posterior alone" and "fixation alone" surgical approaches are currently the preferred modes of treatment for group A basilar invagination.

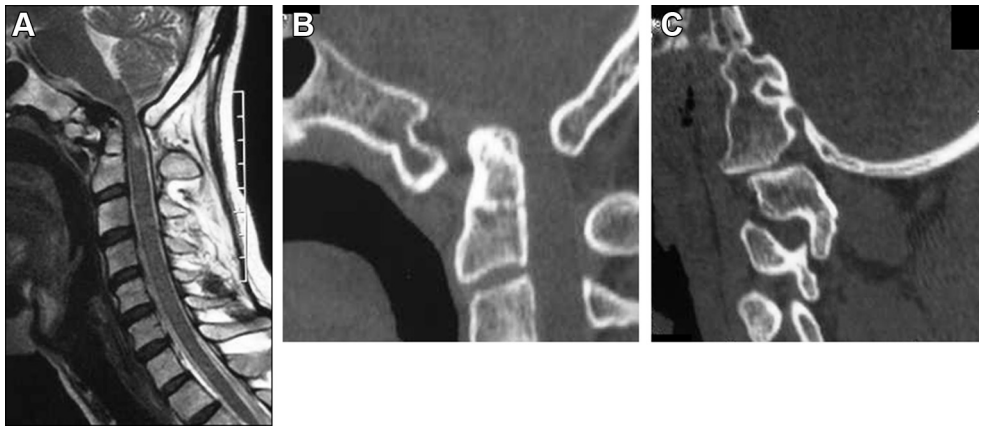

Figure 5. Group A4: images of a 32-year-old male. (**A**) T2-weighted magnetic resonance imaging showing basilar invagination and cord compression. There is no syringomyelia. (**B**) Computed tomography (CT) scan showing basilar invagination and assimilation of atlas. (**C**) CT scan with cut passing through the facets showing type A atlantoaxial facetal instability.

We have evaluated our experience with 510 patients with group A basilar invagination treated over a 9-year period. The aim of the study was to assess the musculoskeletal and soft tissue alterations in group A basilar invagination. We also evaluated whether the bone alterations influenced the nature of neoneural formations, including syringomyelia and Chiari formation. Forty percent of patients in the study cohort were age <21 years. This age group profile is significantly younger than that in the patients with group B basilar invagination that we evaluated in an earlier series.[9] In the present study, the patients in group A2 were relatively younger than the other groups (Table 1).

The fusion of the occipital condyle with the facet of the atlas determined the presence (or absence) of assimilation of the atlas. Two hundred and fifty patients (49%) had assimilation of the atlas, 238 with bilateral assimilation and 12 with unilateral assimilation. Unilateral assimilation of the atlas has been reported only infrequently in the literature. Unilateral assimilation was always associated with torticollis of the neck.

Eighty-six patients (16.8%) had a bifid posterior arch of the atlas. Apart from our recent report, there is no major case series in the literature focusing on evaluating the bifid posterior arch of the atlas. Although it cannot be demonstrated radiologically, the bifid

Table 2. Epidemiologic Parameters

Parameter					Number of Patients
Sex					
Male					344
Female					166
Age Range (years)	**Group A1**	**Group A2**	**Group A3**	**Group A4**	**Total**
1–10	8	26	2	5	41
11–20	32	118	5	7	162
21–30	18	67	16	12	113
31–40	8	48	14	12	82
41–50		47	16	15	78
51–60		20	5	2	27
61–70		4		2	6
71–80				1	1
Mean age (years)	27	18	34	35	

Table 3. Radiologic Parameters

Parameter	Number of Patients (%)
Chiari formation	126/510 (24.7)
Syringomyelia	415/510 (91.17)
Facetal alignment	
Type A atlantoaxial instability	483 (94.7)
Type B atlantoaxial instability	17 (3.3)
Type C atlantoaxial instability	10 (2)
Assimilation of atlas	250/510 (49)
Unilateral	12
Bilateral	238
Bifid arches of atlas	86/510 (16.8)
C2-3 fusion	234/510 (45.8)
Klippel–Feil syndrome	28/510 (5.5)
Atlantodental/clivodental instability	24/300 (8)
Vertical instability	47/300 (15.6)

Table 4. Craniovertebral Parameters

Radiologic Measurements	Group A1, Range (Mean)	Group A2, Range (Mean)	Group A3, Range (Mean)	Group A4, Range (Mean)	Normal, Range (Mean)
Facetal angulation (angle between C1 and C2 facets), degrees	3.1—21 (9.2)	2.7—31.3 (11.17)	2.9—17.1 (9.1)	3.4—28.8 (8.7)	2—12.5 (6.116)
Angle of C1 facet, degrees	12.1—89 (42.44)	13—103.6 (48.2)	1.6—72.9 (35.37)	4.1—72 (35.85)	0—22.8 (8.324)
Angle of C2 facet, degrees	9.8—83.4 (37)	6.5—103.6 (44.1)	0—79.2 (31.92)	1.7—74.2 (29.7)	0—26.2 (10.684)
Basal angle, degrees	130.9—137.5 (134.5)	126.4—151.8 (135.8)	122.2—140 (135.05)	130—145.6 (136.45)	105.7—133.9 (119.8)
Modified omega angle, degrees	61.1—90.7 (71.4)	30.5—79.8 (60.5)	68.5—78.3 (73.4)	62.2—87.4 (71.2)	75—86 (81.1)
Craniovertebral angle, degrees	86.1—115.4 (104.6)	70.6—115.4 (106.9)	90.9—115 (104.7)	102.4—124 (109.9)	121—165.9 (143.4)
Severity of basilar invagination, mm	6—27.4 (5.85)	4.3—24.5 (12.56)	5.6—17.6 (10.8)	5.2—17.3 (11.74)	<5
Torticollis, degrees	82.3—90 (86.35)	63.4—102.2 (70.5)	61.6—87.8 (74.9)	78.6—89.6 (83.8)	90

posterior arch likely opens up on neck flexion and closes on neck extension in an open—close door format.[18] Such movements of the bifid posterior arch of the atlas could act as a dynamic decompressive laminectomy and likely has a protective function for the critical neural structures in the setting of abnormal mobility of the odontoid process.

C2-3 fusion was identified in 234 patients (45.8%). In 201 of these patients, there was assimilation of the atlas. Essentially bone fusions were more common above (assimilation of the atlas) and below (C2-3 fusion) the tip of the odontoid process. Subaxial vertebral bone fusions, termed Klippel—Feil abnormalities,[19] were identified in 28 patients (5.5%) (**Table 2**). Os-odontoideum was identified in 9 patients (1.7%). Os-odontoideum has been associated more frequently with mobile and reducible atlantoaxial instability than with basilar invagination.[18]

In 24 patients (8%), dynamic imaging showed reduction of atlantodental/clivodental interval on neck extension. In 47 patients (15.6%), there was vertical dislocation, wherein the odontoid process migrated rostrally on neck flexion and returned inferiorly either completely (in 25 patients) or partially (in 22 patients) on neck extension.[20] In 229 patients (76.3%), no odontoid process movement or alteration in the atlantodental alignment was identified on dynamic imaging.

Type A facetal malalignment, seen in 483 patients (94.7%), is characterized by facetal listhesis, mimicking lumbosacral listhesis. In 134 patients (26.2%) with type A facetal instability, the facetal surfaces of the atlas and axis were not in direct articular contact with each other, and the facet of the atlas was positioned anterior to the facet of the axis. Such an anatomic malalignment has been referred to previously as atlantoaxial facetal spondyloptosis.[21] Type

Table 5. Musculoskeletal and Neural Parameters

Radiologic Parameter	Group A1, Range (Mean)	Group A2, Range (Mean)	Group A3, Range (Mean)	Group A4, Range (Mean)	Normal, Range (Mean)
Clival height, cm	2.08—4 (3.23)	3.4—5.1 (4.23)	3.19—4.5 (3.9)	3.47—4.7 (4.1)	3.8—5.2 (4.6)
Neck length, cm	8.4—12.1 (10.01)	6.49—11.72 (9.32)	6.25—10.35 (8.62)	8.9—12.76 (9.71)	11—14 (11.9)
Neural length, cm	11.98—18.1 (15.5)	11.68—17.3 (14.9)	12.10—16.66 (15.08)	14.8—17.2 (16)	14—17 (15.71)
Neural girth at the level of tip of odontoid process, mm	4—8.6 (6)	2—8 (4)	3—9 (5.5)	6—9 (8)	9.1—10.8 (9.5)
At C6 level, mm	1.4—4.5 (2.5)	4—9.6 (6.5)	1—5 (3.3)	6—8 (7)	6.9—9.4 (10.9)
At D4 level, mm	3.5—4.6 (4.13)	1.9—6.5 (4.46)	5—5.7 (5.1)	4.5—7 (5.8)	6—7.5 (6.6)
Spinal canal dimension					
At C6 level, mm	12.5—14.8 (14.1)	14.2—15.7 (15.1)	11.6—14.5 (13.4)	11.9—14.6 (13.2)	11—14 (12.78)
At D4 level, mm	11—12.5 (12)	9.5—15.7 (12.71)	10.2—13.6 (12.43)	10.7—14.9 (12.83)	11—13.5 (12.2)
Posterior fossa height, cm	2.87—4 (3.17)	2.6—5 (3.74)	3.25—4.4 (3.77)	3.5—4.29 (3.8)	3—4.7 (3.73)
AP diameter of posterior fossa, cm	8.08—11.43 (9.47)	8.5—11.12 (8.63)	7.74—10 (8.67)	8.6—9.67 (8.81)	7.6—9.7 (8.3)

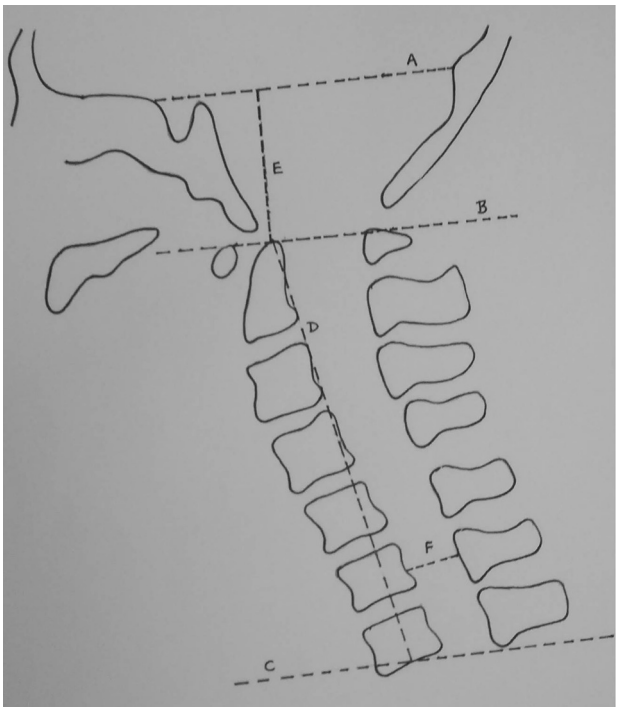

Figure 6. Line drawing used to measure posterior fossa and neck height. With the patient in a neutral head position, a horizontal line (line A) is drawn connecting the tuberculum sellae to the inion. Line B is drawn parallel to line A and courses over the tip of the odontoid process. Line C is drawn parallel to line B and courses over the midpoint of the base of the C7 vertebra. The distance between lines A and B is considered the posterior cranial fossa height, and the distance between lines B and C is considered the neck height.

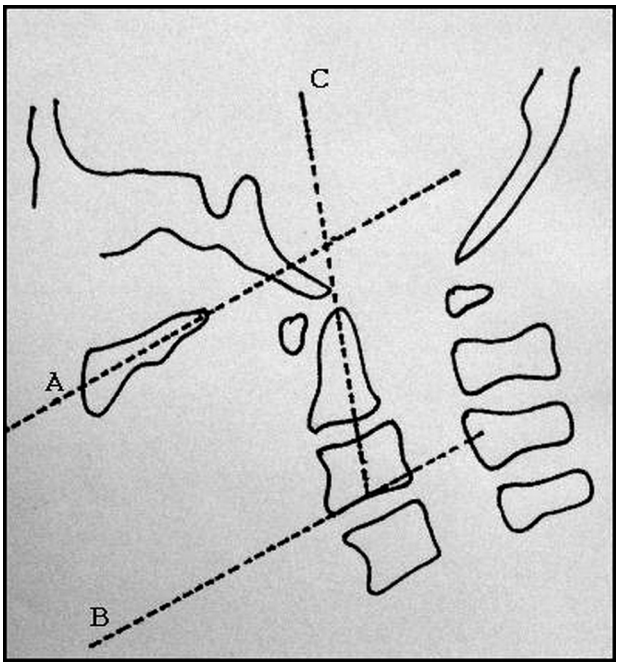

Figure 7. Line drawing ahowing the Goel modified omega angle. Line A is drawn along the line of the hard palate. Line B is drawn parallel to line A, passing through the midpoint of the inferior surface of the C3 vertebral body. Line C is drawn from the midpoint of the inferior surface of the C3 vertebral body and passes through the tip of the odontoid process. The angle between lines B and C is considered the modified omega angle.

B facetal instability, seen in 17 patients (3.3%), is characterized by retrolisthesis of facets. In type C facetal instability, seen in 10 patients (2%), the facets of atlas and axis are in alignment and instability is identified based on corroborative evidence and confirmed by manual manipulation of the bones during surgery. Type B and type C facetal instability were designated central or axial instability. Type A facetal instability is more frequently associated with group A2 and A3 cord abnormalities, whereas type B and C atlantoaxial facetal instability are more often associated with group A1 cord abnormality.[14,15] Atlantoaxial instability is a common denominator irrespective of alterations in alignment seen on dynamic imaging.[7-9,14,15,22,23] The treatment strategy involving facetal manipulation and distraction aimed at craniovertebral realignment and atlantoaxial arthrodesis. Our analysis further concluded that the aim of atlantoaxial stabilization is more paramount than the aim of achieving craniovertebral realignment.

A total of 126 patients (24.7%) had Chiari 1 formation. Our recent studies identified basilar invagination, Chiari formation, and syringomyelia as representing a spectrum of abnormalities in which atlantoaxial instability is the primary etiology. The presence of Chiari formation was not considered a confounding factor in this study. Five patients had Chiari formation with tonsillar herniation on only 1 side, the side contralateral to the indenting odontoid process in patients presenting with torticollis. This form of tonsillar herniation has not been reported previously. We recently reported our experience with patients with group B basilar invagination and identified excessive CSF outside the confines of the spinal cord (or in the extramedullary compartment) in some of them. This excess CSF in the extramedullary compartment, or external syrinx, was related to the combination of the larger spinal canal and thinner spinal cord girth compared with the normal cohort. The total spinal neural girth was measured in the anteroposterior dimension at the C6 and D4 vertebral levels. Spinal neural girth, measured in the presence or absence of syringomyelia, was reduced, and the spinal bony canal was increased in majority of cases compared with the normal cohort.

We used the Chamberlain line and Wackenheim clival lines to measure the degree and nature of basilar invagination,[12,13] and used the Goel modified omega angle to measure the angulation of the odontoid process (Figure 7). To measure the angulation of the odontoid process in transverse or horizontal perspective, we used the inclination of the odontoid process with respect to the bimastoid line. The bimastoid line and bidigastric lines were used to measure basilar invagination in the era when plain radiographs formed the basis of investigation. The use of the bimastoid line to measure the horizontal tilt or inclination of the odontoid process has not been discussed in the literature.

We previously reported using the measurement of brainstem girth opposite the tip of the odontoid process.[6]

In our analysis, the degree of alteration in craniovertebral and odontoid process angulation determined the nature of neural abnormalities (Table 4). The more severe the inclination of the odontoid process (in either the anteroposterior or the horizontal or transverse perspective) and the more acute the craniovertebral angulation, the more frequent the presence of group A2 or A3 cord abnormalities. The type of facetal instability and the degree of angulation of the inferior surface of the facet of the atlas influenced the angulation of the odontoid process and the extent of neural compression. The more severe the inclination of the C1 facet and the more severe the cord compression, the higher the incidence of external syringomyelia.

Although further evaluation is needed, the presence of syringomyelia (group A1), external syringomyelia (group A2), both syringomyelia and external syringomyelia (group A3), or no evidence of unusual CSF loculation (group A4) in the cervical spine could provide clues as to the direction of migration of the odontoid process and degree of basilar invagination and the extent of cord compression. It seems that the pathogenesis of syringomyelia/external syringomyelia is similar in patients with group A and group B basilar invagination and in patients with no bone abnormality at the craniovertebral junction, and is related to inclination of the odontoid process and atlantoaxial instability.

We designated shortening of the clivus as "shortening of the head." Short neck and short head were simultaneous and proportional (Table 5). There was an increase in the size of the spinal canal and a simultaneous and proportionate increase in the anteroposterior dimension of the posterior cranial fossa, along with a reduced girth or atrophy of the spinal cord. Excessive CSF volume was identified even in the posterior cranial fossa compartment. External syringobulbia was seen in all 4 groups, irrespective of the presence of CSF within the cord (syringomyelia), outside the cord (external syringomyelia), or both within and outside the cord (group A3). External syringobulbia was present in 35 of 45 patients (77.7%) in group A4 when there was no significant abnormality of CSF cavitation in the spine. In such cases, the cerebellum was atrophic, and a greater than normal amount of CSF was present around the cerebellum and the brainstem. The role of blockage of CSF pathways related to tonsillar herniation in the pathogenesis of abnormal CSF loculations in the posterior cranial fossa and spine needs to be evaluated.

Despite the fact that the facetal surfaces of the atlas and axis were in an abnormal orientation and inclination, the joint was functional. This finding was verified during the operative procedure, which involved opening the joint. The angle of inclination of the facet of the atlas ranged from 12.1 to 103.6 degrees from horizontal. The angle of the facet of the axis from horizontal ranged from 0 to 103.6 degrees.

In our patients with group A basilar invagination, the neural structures in both the posterior fossa and the cervical spinal cord and both above and below the site of maximum cord compression were atrophic compared with the normal cohort. In addition, the bone compartments housing these neural structures in both the spinal canal and the posterior cranial fossa were vertically reduced in length, resulting in a short neck and a short head, but were increased in dimension anteroposteriorly. Although we could not confirm it owing to an inadequate number of images, the length of the entire spine is likely reduced in these patients compared with the normal cohort. A reduction in neural girth, a decrease in vertical spinal height, an increase in transverse spinal canal dimensions, and an increase in the length of neural structures resulted in an outcome that made the neural structures float in an excessive volume of CSF present either within or outside the neural structures. In this respect, the pathogenesis and function of CSF appeared to be similar regardless of its presence within or outside the neural structures.

CONCLUSION

The degree of basilar invagination and the angulation of the odontoid process are among the key factors determining the presence or absence of syringomyelia or external syrinx formation. Atlantoaxial instability is the primary abnormality in group A basilar invagination.

REFERENCES

1. Shah A, Serchi E. Management of basilar invagination: a historical perspective. *J Craniovertebr Junction Spine*. 2016;7:96-100.
2. Virchow R. *Contributions to the Physical Anthropology of the Germans, with special regard to the Frisians. [Beitrage zur physischen Anthropologie der Deutschen, mit besonderer Berucksichtigung der Friesen]*. Berlin: Abhandlungen de Koniglichen Akademie der Wissenschaften; 1876 [in German].
3. Von Torklus D, Gehle W. *The Upper Cervical Spine: Regional Anatomy, Pathology, and Traumatology. A Systematic Radiological Atlas and Textbook*. New York, NY: Grune & Stratton; 1972:1-98.
4. Grawitz P. Contribution to the teaching of the basilar Impression of the skull. [Beitrag zur Lehre von der basilaren Impression des Schadels]. *Arch Path Anat Physiol*. 1880;80:449-474 [in German].
5. Menezes AH. Primary craniovertebral anomalies and the hindbrain herniation syndrome (Chiari I): database analysis. *Pediatr Neurosurg*. 1995;23:260-269.
6. Goel A, Bhatjiwale M, Desai K. Basilar invagination: a study based on 190 surgically treated cases. *J Neurosurg*. 1998;88:962-968.
7. Goel A. Treatment of basilar invagination by atlantoaxial joint distraction and direct lateral mass fixation. *J Neurosurg Spine*. 2004;1:281-286.
8. Goel A, Nadkarni T, Shah A, Sathe P, Patil M. Radiological evaluation of basilar invagination without obvious atlantoaxial instability (group B basilar invagination): analysis based on a study of 75 patients. *World Neurosurg*. 2016;95:375-382.
9. Goel A, Sathe P, Shah A. Atlantoaxial fixation for basilar invagination without obvious atlantoaxial instability (group B basilar invagination): outcome analysis of 63 surgically treated cases. *World Neurosurg*. 2017;99:164-170.
10. Goel A. Occiput, C1 and C2 instrumentation. In: Winn RH, ed. *Youmans and Winn Neurological Surgery*. Philadelphia, PA: Elsevier; 2017:2643-2655.
11. Goel A, Shah A. Reversal of longstanding musculoskeletal changes in basilar invagination after surgical decompression and stabilization. *J Neurosurg Spine*. 2009;10:220-227.
12. Thiebaut F, Wackenheim A, Vrousos C. [New median sagittal pneumostratigraphical finding concerning the posterior fossa]. *J Radiol Electrol Med Nucl*. 1961;42:1-7 [in French].
13. Chamberlain WE. Basilar impression (platybasia): a bizarre developmental anomaly of the occipital bone and upper cervical spine with striking and misleading neurologic manifestations. *Yale J Biol Med*. 1939;11:487-496.

14. Goel A. Goel's classification of atlantoaxial "facetal" dislocation. *J Craniovertebr Junction Spine*. 2014;5:3-8.

15. Goel A. Facetal alignment: basis of an alternative Goel's classification of basilar invagination. *J Craniovertebr Junction Spine*. 2014;5:59-64.

16. Goel A, Desai KI, Muzumdar DP. Atlantoaxial fixation using plate and screw method: a report of 160 treated patients. *Neurosurgery*. 2002;51: 1351-1356 [discussion: 1356-1357].

17. Goel A, Laheri V. Plate and screw fixation for atlanto-axial subluxation. *Acta Neurochir (Wien)*. 1994;129:47-53.

18. Goel A, Nadkarni T, Shah A, Ramdasi R, Patni N. Bifid anterior and posterior arches of atlas: surgical implication and analysis of 70 cases. *Neurosurgery*. 2015;77:296-305 [discussion: 305-306].

19. David KM, Thorogood PV, Stevens JM, Crockard HA. The dysmorphic cervical spine in Klippel-Feil syndrome: interpretations from developmental biology. *Neurosurg Focus*. 1999;6:e1.

20. Goel A, Shah A, Rajan S. Vertical mobile and reducible atlantoaxial dislocation. Clinical article. *J Neurosurg Spine*. 2009;11:9-14.

21. Goel A, Muzumdar D, Dange N. One stage reduction and fixation for atlantoaxial spondyloptosis: report of four cases. *Br J Neurosurg*. 2006;20:209-213.

22. Goel A. Chiari malformation—is atlantoaxial instability the cause? Outcome analysis of 65 patients with Chiari malformation treated by atlantoaxial fixation. *J Neurosurg Spine*. 2015;22:116-127.

23. Shah A, Sathe P, Patil M, Goel A. Treatment of "idiopathic" syrinx by atlantoaxial fixation: Report of an experience with 9 cases. *J Craniovertebr Junction Spine*. 2017;8:15-21.

Conflict of interest statement: The authors declare that the article content was composed in the absence of any commercial or financial relationships that could be construed as a potential conflict of interest.

Received 19 May 2017; accepted 3 July 2017

Citation: World Neurosurg. (2018) 110:533-543.
http://dx.doi.org/10.1016/j.wneu.2017.07.007

Journal homepage: ***www.WORLDNEUROSURGERY.org***

Available online: ***www.sciencedirect.com***